Surface Science 632 (2015) 9–13

Contents lists available at ScienceDirect

Surface Science

journal homepage: www.elsevier.com/locate/susc

Ultrathin silicatene/silicon-carbide hybrid film on a metal substrate

Bing Yang, Shamil Shaikhutdinov *, Hans-Joachim Freund

Abteilung Chemische Physik, Fritz-Haber Institut der Max-Planck Gesellschaft, Faradayweg 4-6, Berlin 14195, Germany

ARTICLE INFO

Article history:
Received 25 June 2014
Accepted 5 September 2014
Available online 16 September 2014

Keywords:
Graphene
Silicatene
Intercalation
Interface

ABSTRACT

Layered graphene/silica heterostructures may become interesting materials in nanotechnology with yet unknown properties. We have attempted here to intercalate graphene into a silicatene/Ru(0001) interface. The experimental results obtained by x-ray photoelectron spectroscopy, low energy electron diffraction, infrared reflection–absorption spectroscopy, and scanning tunneling microscopy suggest the formation of a well-ordered hybrid structure consisting of a single-layer silicatene on top of a silicon carbide monolayer adsorbed on a metal substrate.

1. Introduction

Thin silica films are one of the key materials in many modern technological applications. Recent progress in fabrication of well-defined, ultrathin silica films on metals opened up opportunities for fundamental studies of silica surfaces [1]. The structural motif of such films is a hexagonal layer of corner-sharing [SiO_4] tetrahedra (so called "silicatene"). A single-layer silicatene is bound to a metal support through Si–O–Metal linkages [2]. When supported on noble metal substrates such as Ru(0001) and Pt(111), a double-layer silicatene is formed which is weakly bound to the support via dispersive forces [3–5]. There are certain topological similarities between silicatene and graphene [6]. Apparently, a high flexibility of the Si – O bonds in silica provides an additional degree of freedom while adopting the most stable structure.

Combining these two (graphene and silicatene) materials in one system could, in principle, result in hybrid structures of yet unknown, but potentially interesting properties. Although there were few attempts to support graphene on a thermally grown SiO_2/Si(111) substrate using lithography techniques [7], interaction of graphene with silicon (silica) has been addressed only recently. Wang et al. [8] observed that Si rapidly diffuses from the multilayer graphene surface to the graphene/SiC(000-1) interface upon heating. The reason the Si intercalated and did not form a new stable SiC layer remained unclear. On the basis of density functional theory (DFT) calculations, Kaloni et al. [9] suggested an intercalation mechanism where Si migrates through atomic defects of the graphene sheet. Using scanning tunneling microscopy (STM) and x-ray photoelectron spectroscopy (XPS), Mao et al. [10] showed that Si intercalating the graphene grown on Ru(0001) not only weakens the interaction of graphene with the metal substrate but also retains its superlative properties. With the aid of DFT calculations and STM, Cui et al. [11] proposed another intercalation mechanism, in which the penetration of Si through the graphene lattice is facilitated by a Si–C exchange process. Recently, Lizzit et al. [12] have reported insulation of epitaxial graphene on Ru(0001) by its sequential exposure to silicon and oxygen, which resulted in an amorphous thin silica film between the graphene and the metal as judged by XPS. However, the atomic structure of the silica formed underneath the graphene was not established. Finally, Huang et al. [13] reported accidental formation of a double-layer silicatene on graphene during chemical vapor deposition of graphene on copper foil. Corresponding DFT calculations suggested that graphene hardly forms covalent bonds with a silica layer, albeit exhibits some stabilizing effects.

The present work was carried out in attempts to fabricate well-defined graphene/silicatene layered structures on a metal substrate. Since silicatenes are commonly prepared on metal supports by oxidation of a Si overlayer at very high temperatures [1], graphene does not survive under these conditions and ultimately decompose via gasification into CO and CO_2. To overcome this issue, it is near at hand to reverse the preparation process and start with silicatene as a substrate for the subsequent deposition of graphene. In particular, our recent studies showed that, similar to graphene/metal systems, the interface between a double-layer silicatene and a Ru(0001) surface can readily be intercalated by metallic atoms [14] as well as gas molecules such as CO and D_2 [15]. In this work, we report on the results only obtained for double-layer silicatene.

* Corresponding author.
E-mail address: shaikhutdinov@fhi-berlin.mpg.de (S. Shaikhutdinov).

http://dx.doi.org/10.1016/j.susc.2014.09.004
0039-6028/

2. Materials and methods

The experiments were performed in an ultra-high vacuum (UHV) chamber equipped with a low energy electron diffraction (LEED), infrared reflection absorption spectroscopy (IRAS), XPS, and STM. The IRA-spectra (Bruker IFS 66v) were recorded using p-polarized light at 84° grazing angle of incidence (resolution 4 cm^{-1}). XP-spectra were obtained with the commercial x-ray (Mg K_α = 1253.6 eV) source and Scienta SES 200 analyzer at normal electron emission (typical resolution 200 meV). The binding energies (BE) of core levels were referenced to the Fermi edge of a Ru substrate.

The bilayer silicatene films were grown on Ru(0001) as described in detail elsewhere [5]. Briefly, silicon is vapor deposited onto oxygen precovered 3O(2 × 2)-Ru(0001) surface at ~100 K, followed by oxidation at ~1200 K in 10^{-6} mbar O_2. Exposure to gases at pressures in the mbar range was performed in a separate cell, connected to the UHV chamber through a gate valve. After the treatment, the cell is pumped out down to 10^{-8} mbar and the sample is transferred back to the UHV chamber. Ethylene (C_2H_4, 99.5%, from Linde) was used as supplied.

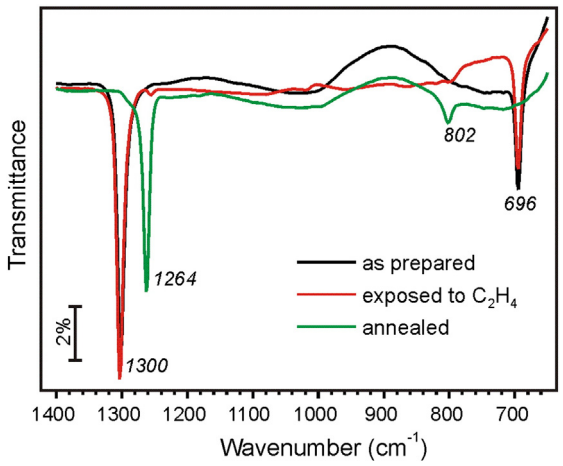

Fig. 2. IRA-spectra of double-layer silicatene: as prepared (black), after exposure to 10 mbar of ethylene at 450 K (red), and subsequent annealing in UHV at 1100 K (green). (For interpretation of the references to color in this figure, the reader is referred to the web version of this article.)

3. Results and discussion

Before we address the results, it is instructive here to recall the characteristic fingerprints of silicatene on metals, in particular on Ru(0001) used here. Single-layer silicatene exhibits the principal IRA-band at 1135 cm^{-1} associated with the stretching of Si – O – Ru linkages [3,5]. The double-layer silicatene shows sharp phonon bands at 1300 cm^{-1} and (a weaker) at 696 cm^{-1}, which are associated with the stretching of Si – O – Si linkages between two silicatene layers and the bending mode of surface Si – O – Si bonds, respectively [3]. All Si ions in silicatene are in the oxidation state 4+ as evidenced by XPS. Compared to the O2p level for oxygen in siloxane (Si – O – Si) bonds, oxygen in Si – O – Ru linkages shows an ~1.5 eV lower binding energy. In addition, the films may contain O atoms directly adsorbed on the Ru(0001) surface [16]. Crystalline silicatene shows (2 × 2)-Ru(0001) diffraction spots in LEED, but forms a diffraction ring (Fig. 1a) for double-layer silicatene in amorphous (glassy) state, both structures often coexisting [17].

For the preparation of graphene layers on metals, decomposition of ethylene or other unsaturated hydrocarbons is commonly used. Exposure of silicatene to ethylene under typical pressures (~10^{-6} mbar) used in UHV chambers caused no considerable changes in IRAS, XPS and LEED, since the siloxane-terminated surface is essentially inert. On the other hand, the exposure at elevated temperatures (~1100 K) resulted in full reduction of the silica layer as no more oxygen was detected in XP-spectra.

Exposure to 10 mbar C_2H_4 for 20 min at 450 K attenuates the LEED pattern considerably (Fig. 1b). The phonon region of the corresponding IRA-spectrum (Fig. 2, red line) shows tiny changes compared to the "as prepared" sample, thus suggesting that the principal structure of silicatene is not affected by this treatment. However, some additional bands are observed in the region between 3000 and 2800 cm^{-1} (as shown in Figure S1(a) in the Supplementary Information) which are characteristic for ν(C – H) stretching modes of adsorbed CH_x species. The presence of carbonaceous species on Ru by XPS is difficult to justify due to overlapping of the $Ru3d_{3/2}$ and C1s signals (see Figure S1(b) in the SI). In agreement with IRAS, XPS results show that the silica stoichiometry is maintained; however, the Si2p and O1s levels are equally, by ~1.9 eV, shifted towards higher BEs as shown in Fig. 3.

Core level shifts are commonly observed for thin oxide films grown on metal substrates (see, for example, ref. [18]). Those are usually explained within the well-known Schottky model of a metal/semiconductor interface, where alignment of the Fermi levels in two materials results in a corresponding Schottky barrier and causes band bending in the oxide film. Although band bending can be neglected for *ultrathin* oxide films, the absolute BE values measured by XPS will depend on the work function of a metal support and the position of a so-called "zero charge point" level [19] used for large-gap semiconductors and insulators, such as silica and alumina. In the absence of considerable structural changes for a weakly bound silica film during gas adsorption, as judged here by IRAS, the BE shifts reflect changes in the work function of a

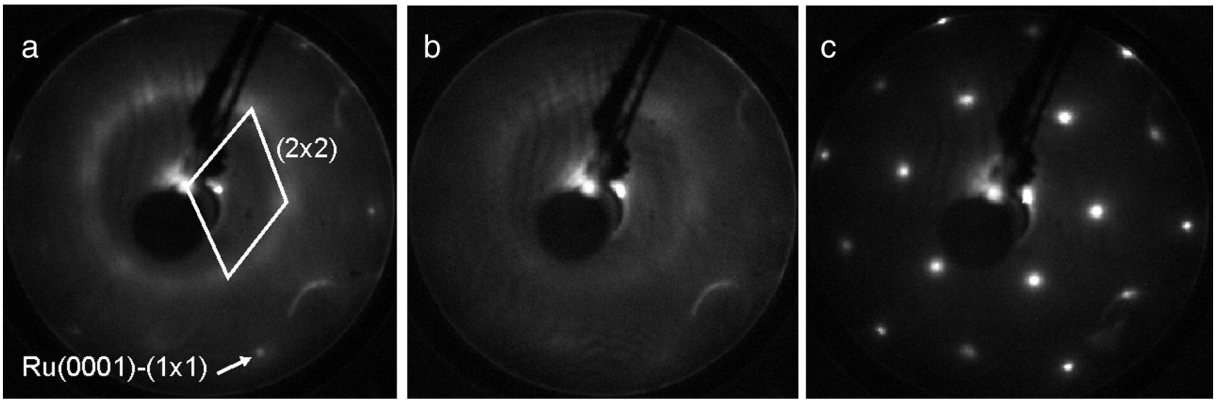

Fig. 1. LEED patterns (60 eV) of double-layer silicatene measured in UHV at 300 K: (a) as prepared; (b) after exposure to 10 mbar of ethylene at 450 K; (c) and subsequent annealing in UHV at 1100 K.

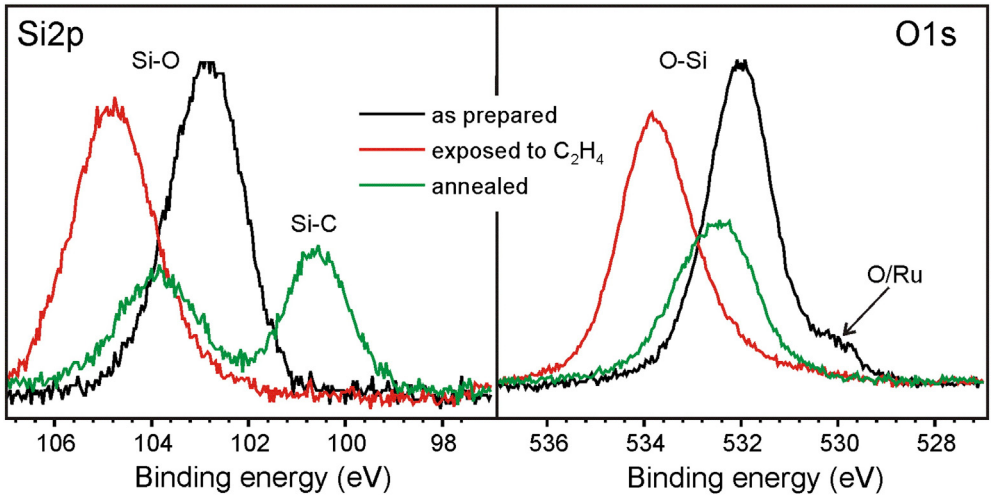

Fig. 3. XP-spectra of the Si2p and O1s levels in double-layer silicatene: as prepared (black), after exposure to 10 mbar of ethylene at 450 K (red), and subsequent annealing in UHV at 1100 K (green). (For interpretation of the references to color in this figure legend, the reader is referred to the web version of this article.)

metal support. Such a behavior has previously been observed for the O atoms directly bonded to the Ru(0001) surface underneath the film [16]. Fig. 3 shows that the signal at 530 eV, associated with the O adatoms on Ru in the "as prepared" sample, disappears upon ethylene exposure. Solely oxygen desorption would cause the BE shift by about 0.8 eV [16] at most, i.e. much smaller than 1.9 eV observed. On the other hand, the shift is very close to the difference in the work functions of the 3O(2 × 2)-Ru(0001) and C/Ru(0001) surfaces (i.e. 6.4 and 4.5 eV, respectively) [20,21]. Therefore, one may conclude that the Ru(0001) surface is covered by carbon (and/or carbonaceous) species upon ethylene exposure at elevated pressures. Certainly, ethylene can only dissociate on the Ru(0001) surface. Ethylene either adsorbs in macroscopic "holes" in the film, thus exposing a Ru(0001) support, or penetrates through the large "pores" in the amorphous silicatene as previously demonstrated for CO [15].

In the next step, the sample was annealed in UHV to the temperatures commonly used for graphene formation on Ru(0001) [22]. Annealing at 1100 K for 3 min resulted in substantial structural changes. Notably, the annealed film became well-ordered, showing sharp (2 × 2) diffraction spots (Fig. 1c). In good agreement with LEED, STM images (Fig. 4) revealed domains with a honeycomb-like structure with a ~5.5 A periodicity, which are separated by defect lines mostly consisting of large depressions assigned to the large N-membered rings [6,23]. No Moire-like superstructures are observed in LEED and STM, otherwise expected for the formation of graphene adsorbed on Ru(0001) [10,11].

The corresponding IRA-spectrum, shown in Fig. 2, revealed a strong band at 1264 cm^{-1} and a weaker band at 802 cm^{-1}, while the original bands at 1302 and 696 cm^{-1} disappeared. XPS inspection of the same sample (Fig. 3) shows that the amount of oxygen is decreased by a factor of ~2, whereas the total amount of Si in the system remains the same, although it splits in two, almost equally populated species. The high BE signal (at ~104 eV) remains assigned to Si in the 4 + state, and its shift may, again, be associated with the work function change. Regarding the low BE signal at ~101 eV, XPS studies available in the literature on Si-based materials allow us to assign this peak to Si cations coordinated to C like in silicon carbide [24–26]. Therefore, the XPS results suggest that about a half of oxygen ions in the silicatene are replaced by carbon upon UHV annealing. The extent of such substitution depends on the ethylene exposure time. In the samples studied, both original and new IR bands showed an inverse relation without substantial shift (see Fig. S2 in the SI). The intensity of new bands is proportional to the amount of Si in the low BE state, i.e. in Si–C environment. These results are indicative for the phase coexistence of the carbon-containing and the pristine silicatene layers, the former expands in area until it covers the whole surface.

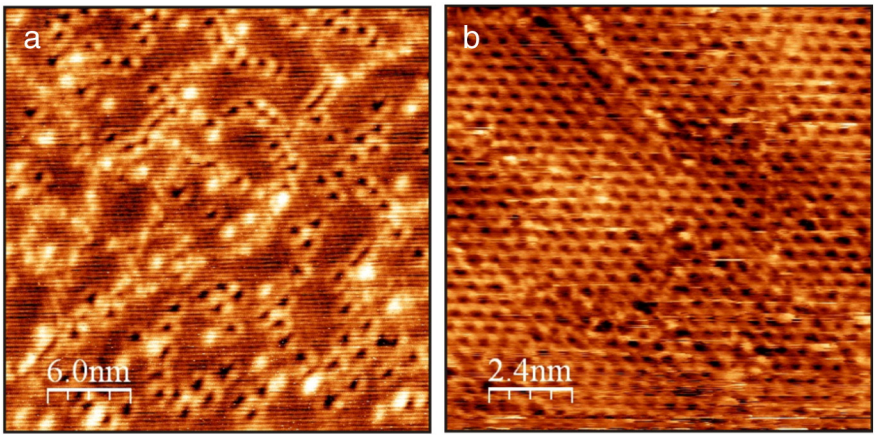

Fig. 4. High-resolution STM images of the silicatene film exposed to 10 mbar of ethylene at 450 K and then annealed in UHV to 1100 K. Sample bias: −3 V (a), −1 V(b), tunneling current 0.1 nA.

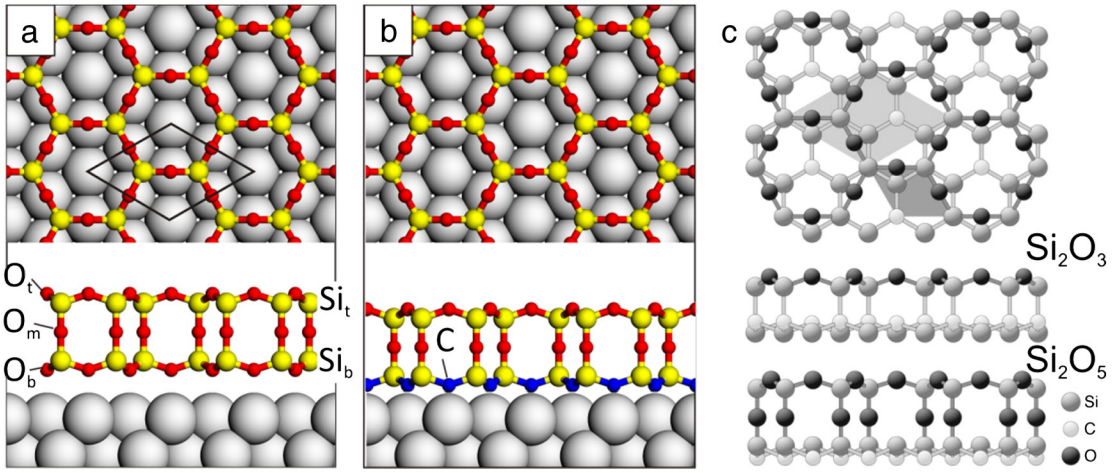

Fig. 5. a) Top and cross views of double-layer silicatene on Ru(0001). The unit cell is indicated. b) Tentative structure of the film prepared in this study (see text for details). c) Top and side views of the Si_2O_3 and Si_2O_5 silicate structures on SiC(0001) as proposed in ref. [28]. Dark and light shaded areas indicate the unit cell of SiC and silica overlayer, respectively.

In double-layer silicatene, there are three non-equivalent oxygen species (see Fig. 5a): O_t and O_b are oxygens in the top and bottom layers coordinated either to Si_t or Si_b cations, respectively; O_m is oxygen linking two single-layer silicatenes thus forming a Si_t–O_m–Si_b linkage. Those oxygen (O_t, O_m, and O_b) species are populated in the ratio 3:2:3 per unit cell. Substitution of O_m atoms by carbon would result in equivalent Si species and oxygen depletion by 25%, thus contradicting the XPS results showing two Si species and oxygen depletion by about 50%. Random distribution of carbon atoms replacing oxygen in top and bottom layers would, again, result in equivalent Si species. Therefore, one has to replace either O_t or O_b species. In this case, oxygen depletion would account 37.5%, i.e. reasonably close to ~50% as observed. Since carbon atoms were adsorbed on the Ru support prior to the UHV annealing, it seems plausible that intercalated carbon reacts with oxygen in the bottom layer, ultimately substituting O_b species. The released oxygen atoms adsorb on the Ru surface and then either recombinatively desorb upon annealing, or react with unreacted carbon atoms to form CO which also desorbs. A higher than expected oxygen depletion (~50% vs 37.5%) in the films could be explained by partial reduction of the silica film by carbon, thus resulting in areas of oxygen-deficient silicon carbide structures.

In principle, the multi-valency of carbon allows all or some C atoms in the bottom layer to form bonds with the Ru surface. This would have a stabilization effect and result in better film ordering as observed by LEED (Fig. 1). Indeed, good crystallinity of single layer silicatenes grown on Mo(112) [2] and Ru(0001) [5] is primarily driven by strong Si – O – Metal bonds leading to an epitaxial registry with a metal surface. Also our recent study of Fe-doped silicate films [27] showed a promotional effect of Fe ions in the bottom layer on film ordering.

This analysis allows us to propose the structure, depicted in Fig. 5b, which fits well the experimental results obtained so far. In fact, the proposed structure is nothing else but a single layer silicatene placed on top of a SiC-like monolayer formed on Ru(0001). Beside the above-discussed arguments based on LEED and XPS data, the proposed structure agrees well with the IRAS results showing that the Si–O–Si linkage is essentially maintained, as the corresponding stretching frequency at 1300 cm^{-1} is only by 35 cm^{-1} red-shifted. It is noteworthy that another band (at 802 cm^{-1}) is close to the one at 790 cm^{-1}, observed for a single-layer silicatene on Ru(0001) and associated with asymmetric stretching of Si – O – Ru linkage combined with O – Si – O bending mode. The latter finding is also consistent with the proposed model, suggesting a stronger bonding of the bottom layer to the metal support as compared to pristine double-layer silicatene.

The model, depicted in Fig. 5b, is very similar to those proposed by Heinz and coworkers [28] for ultrathin silica films grown on SiC(0001), shown in Fig. 5c for comparison. Depending on surface termination of SiC, i.e. either C or Si, two structures were suggested on the basis of I/V LEED measurements. Further DFT study [29] showed that in the case of C-terminated surface, both the Si_2O_3 and the Si_2O_5 models have roughly the same formation energy, whereas the Si_2O_5 model is energetically much more favorable on the Si-terminated surface. The DFT-calculated structural parameters were in excellent agreement with the LEED results.

4. Conclusions

In attempts to intercalate graphene into a silicatene/Ru(0001) interface, we have fabricated a well-ordered hybrid structure consisting of a single-layer silicatene on top of a silicon carbide monolayer adsorbed on a metal substrate. The structure reported here may be interesting for metal/oxide/semiconductor (MOS) systems. The formation of a high quality oxide layer on SiC is a key requirement for MOS devices based on this material [30,31]. In addition, thin films of silicon oxycarbides, i.e. having Si coordinated both to C and O, were shown to exhibit many interesting, particularly optical, properties [32,33]. We believe that the observed hybrid structure may provide a basis for development of new generation two-dimensional systems with unique properties.

In addition, the results show that fabrication of sandwiched graphene/silicatene structures on a metal substrate seems to be hardly possible by synthesis based on an *intercalation* approach. Perhaps, sedimentation of graphene and silicatene "flakes" could be more feasible for those objectives. However, in contrast to graphene, reliable preparation of free-standing silicatene remains unknown.

Acknowledgments

The authors gratefully acknowledge the financial support by the Deutsche Forschungsgemeinschaft (DFG) through Collaborative Research Center 1109 and the Fonds der Chemischen Industrie.

Appendix A. Supplementary data

Supplementary data to this article can be found online at http://dx.doi.org/10.1016/j.susc.2014.09.004.

References

[1] S. Shaikhutdinov, H.-J. Freund, Adv. Mater. 25 (2013) 49.
[2] J. Weissenrieder, S. Kaya, J.-L. Lu, H.-J. Gao, S. Shaikhutdinov, H.-J. Freund, M. Sierka, T.K. Todorova, J. Sauer, Phys. Rev. Lett. 95 (2005) 076103.
[3] D. Löffler, J.J. Uhlrich, M. Baron, B. Yang, X. Yu, L. Lichtenstein, L. Heinke, C. Büchner, M. Heyde, S. Shaikhutdinov, H.J. Freund, R. Włodarczyk, M. Sierka, J. Sauer, Phys. Rev. Lett. 105 (2010) 146104.
[4] X. Yu, B. Yang, J.A. Boscoboinik, S. Shaikhutdinov, H.-J. Freund, Appl. Phys. Lett. 100 (2012) 151608.
[5] B. Yang, W.E. Kaden, X. Yu, J.A. Boscoboinik, Y. Martynova, L. Lichtenstein, M. Heyde, M. Sterrer, R. Wlodarczyk, M. Sierka, J. Sauer, S. Shaikhutdinov, H.-J. Freund, Phys. Chem. Chem. Phys. 14 (2012) 11344.
[6] B. Yang, J.A. Boscoboinik, X. Yu, S. Shaikhutdinov, H.-J. Freund, Nano Lett. 13 (2013) 4422.
[7] M. Ishigami, J.H. Chen, W.G. Cullen, M.S. Fuhrer, E.D. Williams, Nano Lett. 7 (2007) 1643.
[8] F. Wang, K. Shepperd, J. Hicks, M.S. Nevius, H. Tinkey, A. Tejeda, A. Taleb-Ibrahimi, F. Bertran, P. Le Fèvre, D.B. Torrance, P.N. First, W.A. de Heer, A.A. Zakharov, E.H. Conrad, Phys. Rev. B 85 (2012) 165449.
[9] T.P. Kaloni, M.U. Kahaly, Y.C. Cheng, U. Schwingenschlogl, J. Mater. Chem. 22 (2012) 23340.
[10] J. Mao, L. Huang, Y. Pan, M. Gao, J. He, H. Zhou, H. Guo, Y. Tian, Q. Zou, L. Zhang, H. Zhang, Y. Wang, S. Du, X. Zhou, A.H. Castro Neto, H.-J. Gao, Appl. Phys. Lett. 100 (2012).
[11] Y. Cui, J. Gao, L. Jin, J. Zhao, D. Tan, Q. Fu, X. Bao, Nano Res. 5 (2012) 352.
[12] S. Lizzit, R. Larciprete, P. Lacovig, M. Dalmiglio, F. Orlando, A. Baraldi, L. Gammelgaard, L. Barreto, M. Bianchi, E. Perkins, P. Hofmann, Nano Lett. 12 (2012) 4503.
[13] P.Y. Huang, S. Kurasch, A. Srivastava, V. Skakalova, J. Kotakoski, A.V. Krasheninnikov, R. Hovden, Q. Mao, J.C. Meyer, J. Smet, D.A. Muller, U. Kaiser, Nano Lett. 12 (2012) 1081.
[14] W.E. Kaden, C. Büchner, L. Lichtenstein, S. Stuckenholz, F. Ringleb, M. Heyde, M. Sterrer, H.-J. Freund, L. Giordano, G. Pacchioni, C.J. Nelin, P.S. Bagus, Phys. Rev. B 89 (2014) 115436.
[15] E. Emmez, B. Yang, S. Shaikhutdinov, H.J. Freund, On the Permeation of a Single Layer SiO_2 Membrane and Chemistry in Confined Space, J. Phys. Chem. C, http://dx.doi.org/10.1021/jp503253a.
[16] R. Włodarczyk, M. Sierka, J. Sauer, D. Löffler, J.J. Uhlrich, X. Yu, B. Yang, I.M.N. Groot, S. Shaikhutdinov, H.J. Freund, Phys. Rev. B 85 (2012) 085403.
[17] M. Heyde, S. Shaikhutdinov, H.J. Freund, Chem. Phys. Lett. 550 (2012) 1.
[18] Y. Wu, E. Garfunkel, T.E. Madey, Surf. Sci. 365 (1996) 337.
[19] C. Noguera, Physics and Chemistry at Oxide Surfaces, Cambridge University Press, 1996.
[20] F.J. Himpsel, K. Christmann, P. Heimann, D.E. Eastman, P.J. Feibelman, Surf. Sci. 115 (1982) L159.
[21] Y.D. Kim, A.P. Seitsonen, S. Wendt, J. Wang, C. Fan, K. Jacobi, H. Over, G. Ertl, J. Phys. Chem. B 105 (2001) 3752.
[22] H. Zhang, Q. Fu, Y. Cui, D. Tan, X. Bao, J. Phys. Chem. C 113 (2009) 8296.
[23] L. Lichtenstein, C. Büchner, B. Yang, S. Shaikhutdinov, M. Heyde, M. Sierka, R. Włodarczyk, J. Sauer, H.-J. Freund, Angew. Chem. Int. Ed. 51 (2012) 404.
[24] I. Kusunoki, Y. Igari, Appl. Surf. Sci. 59 (1992) 95.
[25] A. Santoni, R. Frycek, P. Castrucci, M. Scarselli, M. De Crescenzi, Surf. Sci. 582 (2005) 125.
[26] M. Schürmann, S. Dreiner, U. Berges, C. Westphal, Phys. Rev. B 74 (2006) 035309.
[27] R. Włodarczyk, J. Sauer, X. Yu, J.A. Boscoboinik, B. Yang, S. Shaikhutdinov, H.-J. Freund, J. Am. Chem. Soc. 135 (2013) 19222.
[28] J. Bernhardt, J. Schardt, U. Starke, K. Heinz, Appl. Phys. Lett. 74 (1999) 1084.
[29] W. Lu, P. Krüger, J. Pollmann, Phys. Rev. B 61 (2000) 13737.
[30] C. Raynaud, J. Non-Cryst. Solids 280 (2001) 1.
[31] V. Presser, K.G. Nickel, Crit. Rev. Solid State Mater. Sci. 33 (2008) 1.
[32] S. Gallis, V. Nikas, H. Suhag, M. Huang, A.E. Kaloyeros, Appl. Phys. Lett. 97 (2010) 081905-4.
[33] C. Pantano, A. Singh, H. Zhang, Journal of Sol–gel Sci. Technol. 14 (1999) 7.